RSC Advances

ROYAL SOCIETY OF CHEMISTRY

www.rsc.org/advances

Physical Chemistry Chemical Physics

Dynamic Article Links ►

Cite this: DOI: 10.1039/c0xx00000x

ARTICLE TYPE

www.rsc.org/xxxxxx

Valence and Rydberg states of CH_3Cl: A MR-CISD study

Vanessa C. de Medeiros[a], Silmar A. do Monte[a] and Elizete Ventura*[a]

In this work ten singlet and nine triplet states are studied through multi-reference configuration interaction with singles and doubles (MR-CISD), including Davidson extensivity correction (MR-CISD+Q). For the first time the excited states whose energies are larger than ~ 9.5 eV have been calculated using highly correlated methods. The energies, spatial extent ($<r^2>$), configurations weights and oscillator strengths (*f*) have been computed. At the MR-CISD+Q level the excited states energies vary from ~ 7.51 to 11.98 eV. The lowest (nσ*) excited singlet state is significantly mixed with the $n3p_{a1}$ and n3s Rydberg states, while the next (n3s) has a non-negligible mixture with the nσ* state. The next three singlet states obtained result from the $(n_{Cl})^3(3p_e)^1$ configuration and are almost degenerate. The next ($n3p_{a1}$) singlet state is significantly mixed with the nσ* state, while the last three have $\sigma_{C\text{-}Cl} \rightarrow$ Rydberg (3s or 3p) as the main configurations. According to the *f* values the most intense transition is to the 4^1A_1 state, a $\sigma 3p_{a1}$ Rydberg state mixed with the σσ* and σ3s configurations. Our results indicate that the σσ* configuration is responsible for the high *f* value of the gs $\rightarrow 4^1A_1$ transition. The Rydberg-valence mixing is greatly reduced in the triplet states whose singlet counterparts have significant multiconfigurational character. The 2^3A_1 state (σσ*) does not have its singlet counterpart, while the 4^1A_1 state ($\sigma 3p_{a1}$ + σσ* + σ3s) does not have its triplet counterpart. The obtained results are in good agreement with experimental results and with previous CASPT2 results.

Introduction

CH_3Cl is one of the most abundant halocarbons and is estimated that it contributes with ~ 16 % to the Cl atoms in the stratosphere[1]. It is well known that Cl atoms catalyses O_3 decomposition[2]. A very significant percentage of CH_3Cl comes from natural sources[3], making it a particularly important compound.

Some photodissociation channels of clorofluorcarbons (CFCs) and halocarbons involve excitation from chlorine lone pairs (*n*) to C – Cl antibonding (σ*) orbitals[4-6] and lie in the UV region[7]. Although a large percentage of these molecules photodissociate while in the stratosphere, the surviving molecules can reach the ionosphere, where vacuum UV (VUV) is present, and in this case the Rydberg states play a very important role[8]. Thus, a detailed knowledge of its excited states is of fundamental importance to understand its photochemistry.

The photoabsorption spectrum of CH_3Cl has been studied by several authors (see, for instance, refs. 9-13). Four main characteristics can be found in this spectrum: (i) a very weak and relatively broad band between ~ 6.8 and 7.5 eV; (ii) many sharp and intense peaks in the region from ~ 8.7 to 11.3 eV; (iii) a relatively broad and intense band from ~ 10 to 12 eV overlapped with the peaks in (ii); (iv) a very broad and intense band above ~ 12 eV. The broad bands are consistent with transitions from bonding or to antibonding orbitals. However, the latter two broad bands are also expected to underlie Rydberg states.

The neutral CH_3Cl has C_{3v} geometrical structure, and its ground state electron configuration can be represented as [14] $(Core)(5a_1)^2(6a_1)^2(1e)^4(7a_1)^2(2e)^4(8a_1)^0$, where $7a_1$, $2e$, and $8a_1$ correspond to bonding σ(C-Cl), nonbonding *n*(Cl, $3p_x$, $3p_y \equiv 3p_e$) and antibonding σ*(C-Cl) orbitals, respectively. In the ground state geometry the Rydberg orbitals have higher energies than the σ*(C-Cl) orbital. Thus, it is expected that the some valence states are associated with $n \rightarrow \sigma^*$ and $\sigma \rightarrow \sigma^*$ excitations, while some Rydberg states are expected to be associated with $n \rightarrow Ryd$ and $\sigma \rightarrow Ryd$ excitations, in which *Ryd* represent a set of Rydberg orbitals.

In many cases the energies of Rydberg states can be estimated through the Rydberg formula[15-17]:

$$\Delta E = IE - Z/2(n - \delta_l)^2 \quad (1)$$

where Z, ΔE and IE are the charge of the ionic core (1 for neutral molecules), vertical excitation and ionization energies, respectively (in Hartrees), and n and δ_l are the quantum number and the quantum defect, respectively. In Eq. (1), the *l* subscript indicates the main dependence of the quantum defect on the quantum number *l*. As can be seen from this equation the energies of Rydberg states for each series (e.g. *s, p, d*, …) converge to the corresponding ionization energy as *n* increases. The IE value to be used in eq. (1) refers to that orbital from which the electron is excited. In the present case the first two IE values (11.32 and 13.40 eV [18]) are associated with the Cl lone pairs and with the C

– Cl σ orbital, respectively [14, 19]. The type of Rydberg orbital will dictate the n and δ_l values to be used in Eq. (1).

The purpose of the present paper is to describe (singlet and triplet) valence and Rydberg states of the CH_3Cl molecule associated with excitations from the Cl lone pairs and C – Cl σ orbitals. In this way it is possible to extend previous theoretical calculations to include states up to ~ 12 eV. Only *s* and *p* Rydberg states are considered.

Computational Details

The experimental geometry[20] of the CH_3Cl molecule has been used in all calculations. Cs symmetry has been used, and the symmetry plane corresponds to the yz plane. The C – Cl bond almost coincides with the z axis. Therefore, the $3p_z$ lone pair orbital of the Cl atom is involved in the formation of the σ and σ* molecular orbitals. The ($3p_x$, $3p_y$) degenerate pair is designed as 3pe or *n*, yielding the *n*σ* configuration. The 3s(C), $3p_z$(C) and 3pe(C) Rydberg orbitals have also been included in the present study. Although there is a third row atom (Cl) in the molecule the n = 3 notation has been chosen on the basis of the localization of the low Rydberg orbitals in the CH_3 moiety and agrees with that of Rogers *et al.*[21]. Besides, the Rydberg orbitals shapes are similar to those of the protonated formaldehyde obtained by Antol *et al.*[22].

For the MCSCF calculations a valence CAS with six electrons (four from the two lone pairs Cl orbitals and two from the C – Cl sigma bond) and four orbitals (the 3pe(Cl) along with the σ and σ* orbitals) was used. Four additional Rydberg orbitals (3s(C), $3p_{a1}$(C) and 3pe(C)) have been included in the auxiliary (AUX) space and up to three electrons were allowed from the CAS into the AUX orbitals. Preliminary tests performed by our group show that the Rydberg-valence mixing at the MCSCF level is almost independent on the maximum CAS → AUX excitation level. However, very smooth potential energy curves have been obtained, at the MCSCF level, if one includes up to triple excitations from the CAS to the AUX space. Thus, such latter excitation level has been chosen for the MCSCF calculations performed in the present manuscript. Ten singlet states have been included in the state-averaged MCSCF calculations with equal weights for all states. Nine triplet states were treated separately in the state averaging procedure. As Cs symmetry is used in all calculations and the actual symmetry is C_{3v} one needs to compute the average energy of the correct pairs of states to get the energies of the doubly degenerate E states. The same holds for the $\langle r^2 \rangle$ values, while in the case of oscillator strength the individual values in each pair should be summed. The 1^1E, 2^1E, 3^1E, 4^1E and 5^1E states correspond to the $2^1A'/1^1A''$, $3^1A'/2^1A''$, $5^1A'/3^1A''$, $6^1A'/5^1A''$ and $9^1A'/6^1A''$ pairs of states, respectively. In the case of the triplet states one has the same number of E states, but the corresponding roots of A′ symmetry vary from 1 to 8, while those of A″ symmetry vary as they do for the singlet states. The 1^1A_1, 2^1A_1, 1^1A_2, 3^1A_1 and 4^1A_1 states correspond to the $1^1A'$, $4^1A'$, $4^1A''$, $7^1A'$ and $8^1A'$ states, respectively, while in the case of the 1^3A_1, 1^3A_2, 2^3A_1 and 3^3A_1 states the corresponding states in Cs symmetry are $3^3A'$, $4^3A''$, $6^3A'$ and $7^3A'$. In order to verify how the inclusion of high energy states (that is, the states whose energies are greater than 10 eV) affect the properties of the low lying ones the calculations were repeated including seven states in the state-averaging MCSCF procedure for both singlet and triplet states. Such tests are based on the fact that additional Rydberg states (not included in the actual calculations) are predicted above the seventh singlet (4^1E) state here considered, as will be discussed later.

For the multi-reference CI calculations with singles and doubles (MR-CISD) the configuration state functions (CSFs) were generated as in the MCSCF calculations, except that only single CAS → AUX excitations were allowed. The total CSF space was constructed by applying single and double excitations from all internal (active plus doubly occupied) orbitals into all virtual orbitals. The $K + L$ shells orbitals of Cl atom along with the K shell orbital of C atom were kept frozen in all CI calculations. Freezing $K + L$ shells for the Cl atom are based on tests performed for the CF_3Cl molecule[5]. The interacting space restriction[23] was used in all MR-CISD calculations.

Size-extensivity corrections have been considered by means of the generalized Davidson method (MR–CISD + Q)[24,25]. The COLUMBUS program system[26-29] was used for all calculations. The atomic orbitals (AO) integrals and AO gradient integrals were computed with program modules taken from DALTON[30]. The basis set used consists of aug–cc–pVTZ for H and Cl[31,32] and d–aug–cc–pVTZ basis set for C[33,34]. Such choice of a doubly-augmented (d-aug) basis set centered on C atom was based on preliminary calculations concerning potential energy curves of Rydberg states along the C–Cl bond: smooth and continuous curves are obtained if the d-aug basis set is centered on C or on both C and Cl atoms. In both cases the Rydberg orbitals become more localized on CH_3 fragment as the C–Cl bond distance increases, which explains the discontinuous curves obtained when the d-aug basis set is centered only on the Cl atom. Besides, the Rydberg orbitals of the dissociated molecule are very similar to those of the isolated methyl fragment. These results indicate that the Rydberg states are indeed located in the methyl fragment, and the results presented in refs.[35-38] concerning this fragment suggest that the C atom is the Rydberg center.

Additional calculations using the mixed Dunning-Hay DZP + Rydberg" basis set[39,40] for C and aug-cc-pVTZ basis set for the other atoms have also been carried out for the singlet states. The former basis set has been taken from MOLPRO software[41].

Results and Discussion.

In Table 1 the obtained energies, $\langle r^2 \rangle$ (= $\langle x^2 \rangle$ + $\langle y^2 \rangle$ + $\langle z^2 \rangle$) values and oscillator strengths (*f*, at the MR-CISD level) for the studied singlet states are shown. As can be seen from this table the $\langle r^2 \rangle$ values at the MCSCF level already show the significant larger diffuseness of the Rydberg states as compared to the ground state. However, the nature of 1^1E, 2^1E, 4^1E and 4^1A_1 states change as dynamic electron correlation is included. Thus the assignments change accordingly. For instance, at the MCSCF level the 1^1E state would be classified as a n3s state, while at the MR-CISD level it should be classified as a (nσ*) state mixed with ($n3pa_1$) and (n3s) (see Table 1). On the other hand, the 2^1E state would be classified as a ($n3p_z$) + (nσ*) state at the MCSCF level, while at the MR-CISD level it should be classified as a n3s state (see Table 1). Such states' ordering change is likely to be induced by the Rydberg-valence mixing, as the dynamic correlation effect is larger for the valence components than for the Rydberg ones,

due to the smaller number of correlated electrons in the latter. A similar change of nature for these states has been observed by Nachtigallova *et al*. at the CASSCF and CASPT2 levels[10]. Only for the 4^1E state one has the same major configurations at both MCSCF and MR-CISD levels, but the relative weights change (see Table 1). On the other hand, for the 1^1E state the nσ* and $n3p_z$ configurations are important only at the MR-CISD level, while for the 2^1E and 4^1A_1 states the same holds for the n3s and σσ* configurations, respectively (see Table 1). A similar behavior has also been found for the HCFC-133a[42] molecule.

As can be also seen from Table 1 the wavefunctions of several states have a significant multiconfigurational character, even at the MR-CISD level. The largest multiconfigurational characters have been obtained for the1^1E and 4^1A_1 states, with a very large Rydberg-valence mixture (see Table 1). Interestingly, the three states resulting from the $n^1(3pe)^3$ configuration, that is, 2^1A_1, 3^1E and 1^1A_2, have a negligible multiconfigurational character at both MCSCF and MR-CISD levels (see Table 1).

Table 1. MCSCF, MR-CISD and MR-CISD+Q results for the singlet states of the CH_3Cl molecule, calculated with the mixed aug-cc-pVTZ(H,Cl)/d-aug-cc-pVTZ(C) basis set.

state						vertical excitation energies[a]					
						MCSCF	MR-CISD	MR-CISD+Q		Previous theoretical results	
	weigths (MCSCF)[b]	$\langle r^2 \rangle$[c]	weigths (MR-CISD)[b]	$\langle r^2 \rangle$[c]	E_{tot}[d]	-499.129955	-499.518710	-499.565633	expt[e]	CASPT2[f]	MCCEPA[g]
1^1A_1	0.97gs	39.24	0.86gs	42.04	f(x10^3)[h]	0.00	0.00	0.00	---	---	---
1^1E	0.92(n3s)	84.19	0.56(nσ*) +0.17(n3pa_1)+0.15(n3s)	66.05	1.85 (5.74-7.77)[i]	6.72	7.49	7.51	7.25[j]	7.61	7.80
2^1E	0.58(n3pa_1)+0.35(nσ*)	94.29	0.73(n3s)+ 0.13(nσ*)	77.04	60.41 (45.93-62.13)[i] [56][g]	7.13	7.74	7.89	7.75[j]	7.69	8.88
2^1A_1	0.98(n3pe)	116.33	0.88(n3pe)	113.83	4.29 [25][g]	7.58	8.66	8.88	8.82[j]	8.79	8.11
3^1E	0.98(n3pe)	115.98	0.89(n3pe)	113.88	22.09 [110][g]	7.60	8.67	8.90	8.89[j]	8.92	9.00
1^1A_2	0.98(n3pe)	116.34	0.88(n3pe)	114.26	0.00 [0][g]	7.63	8.72	8.95		8.98	9.47
4^1E	0.61(nσ*)+0.38(n3pa_1)	76.31	0.69(n3pa_1)+0.18(nσ*)	112.21	40.88 (86.11-116.50)[i] [18][g]	8.94	9.21	9.31	9.20[j]	9.13	---
3^1A_1	0.85(σ3s)+0.12(σ3pa_1)	87.89	0.71(σ3s)+0.12(σ3pa_1)	84.15	30.75	10.15	10.86	10.96	---	---	---
4^1A_1	0.74(σ3pa_1)+0.14(σ3s)	110.77	0.48(σ3pa_1)+0.22(σσ*) +0.17(σ3s)	92.59	340.28	10.75	11.39	11.40	11.64[k]	---	---
5^1E	0.99(σ3pe)	115.85	0.88(σ3pe)	113.20	34.57	10.97	11.83	11.98	11.75[k]	---	---

[a]in eV; [b]Configurations whose weights are lower than 0.1 were not included; [c]$\langle r^2 \rangle$ expectation values in au; [d]Ground-state energy in hartrees; [e]experimental results; [f]ref. [10]; [g]ref. [11]; [h]Oscillator strengths (*f*) calculated at MR-CISD level; [i]experimental range modified from that of ref. [45]. See text for details; [j]ref. [9]; [k]ref. [12];

Many members of the Rydberg series are predicted above the here studied 4^1E state. For instance, if one uses a value of 0.01 for the quantum defect[21,43] of carbon *d* orbitals the Rydberg formula (Eq. 1) predicts a n3d Rydberg state at ~ 9.77 eV. The n4s and n4p Rydberg states are predicted at ~ 9.80 and 10.13 eV, respectively. Additional members with higher *n* values are predicted below the first ionization potential (see Eq. (1)), although their intensities are expected to decrease steeply as the principal quantum number increases[44]. It is important to mention that the accuracy of such predictions depends on the absence of Rydberg-valence mixing[16]. As these orbitals (and the associated configurations) can affect the highest lying (3^1A_1, 4^1A_1, and 5^1E or 3^3A_1 and 5^3E in the case of triplet states) states here studied and as they have not been included in the calculations, due to the prohibitively high computational effort involved, a lower accuracy is expected for these highest lying states, as compared to the lower lying ones. However, to the best of our knowledge there are no other highly correlated theoretical results concerning excited states of CH_3Cl above ~ 9.5 eV. Thus, our results cannot be compared with other theoretical results in this energy range.

The quantum defect values, estimated from Eq.(1) along with the highest level excitation energies values (MR-CISD+Q) provided in Table 1, are ~ 1.01 and 0.62 (average value obtained from the 2^1A_1, 3^1E and 1^1A_2 states) for the n3s and n3pe states, respectively, which can be compared to the corresponding values of 0.98 and 0.58 for the 3s and 3p states of the C atom[21]. For the 4^1E state the predicted value of ~ 0.40 deviates significantly from that expected for a 3p state of C atom, which can be due to the admixture between the n3pa (Rydberg) and nσ*(valence) configurations and to the non-negligible (though small) weight of the σ orbital in the $3pa_1$ orbital. For the remaining states the ionization energy of 13.40 eV (associated with ionization of C – Cl σ orbital) should be used. In the case of the 3^1A_1 state the predicted value of ~ 0.64 is slightly higher than the previous one (0.62), which can be explained by a small contribution of a 3p state (see Table 1). On the other hand, for the 4^1A_1 state the significant admixture between valence and Rydberg states leads to a value of ~ 0.39, which differ significantly from the value of 0.58 for a 3p state. The excitation energy obtained for the 4^1E (11.98 eV) does not agree at all with the value predicted by the Rydberg's formula for a 3p state, ~ 11.08 eV. However, the value of 11.98 eV is relatively close to the value predicted for a 4p state (~12.24 eV). Thus, such discrepancy can be explained by a possible contribution of a 4p state, not enclosed by the actual calculations.

As can be seen from Table 1 for the states whose nature do not change as dynamic electron correlation is included such effect in the excitation energies is large, leading to increases from 0.64 to 1.09 eV. The effect of dynamic electron correlation at the CASPT2 level is also large, but in this case the excitation energies decrease[10]. Upon inclusion of extensivity correction at the MR-CISD + Q level all excitation energies increase by at most 0.23 eV. This largest increase has been obtained for the 3^1E and 1^1A_2 states (see Table 1). A similar effect has been obtained for the CF_3Cl molecule[5], although in that case the maximum increase for the singlet states is 0.16 eV.

Our results for the excitation energies at the MR-CISD+Q level are in good agreement with previous CASPT2 results[10], with a maximum difference of ~ 0.2 eV, obtained for the 2^1E state (see Table 1). However, there is a discrepancy between our results and the results of Cossart-Magos *et al*., obtained at the multiconfiguration coupled electron pair approximation (MCCEPA) level[11], that is, according to their results the 3^1E state is lower in energy than the 2^1A_1 state. Thus, our result for the former state is ~ 0.79 eV higher in energy (see Table 1). There is also good agreement between our MR-CISD+Q results and the experimental results from refs. 9 and 12, with a maximum difference of 0.26 eV, obtained for the 1^1E state (see Table 1). However, in the case of the peak at 8.90 eV we suggest a different assignment from that of reference 9. While the authors assign it as a $n4pa_1$ state whose Rydberg series converge to the $^2E_{1/2}$ state of the cation we alternatively assign it as a n3pe state (see Table 1), as the relative intensities of the two peaks (at 8.82 and 8.89 eV[9]) are not compatible with a small spin-orbit coupling expected for this molecule[5]. Besides, if one compares the intensities of the pair of peaks at 9.2 and 9.32 eV (assigned as n4pe states by the authors, see fig. 2b of ref. 9), which converge to the $^2E_{3/2}$ and $^2E_{1/2}$ states of the cation, respectively, is clear that the intensity of the latter is much lower than that of the former, which is compatible with a small spin-orbit coupling. In the case of the pair of peaks around 7.8 eV (corresponding to n4s transitions) the broadness of the band prevents even a qualitative comparison between the intensities of the two peaks (see fig. 2a of ref. 9). As there is a large density of states near 11 eV[12] we were not able to compare the state calculated at 10.96 eV to a experimental peak. The 4^1A_1 state (at 11.40 eV) was compared to a maximum of a very broad band, while the next state (5^1E) was compared to a slight shoulder located at 11.75 eV (see Table 1).

Another important differences between our results and that from ref. 11 are the following: (i) the 2^1E and 3^1E states are highly coupled (what can be explained by their close energies) and mainly composed of the … $2e^3 4s^1$ and … $2e^3 4pa_1^1$ configurations. Apart from the different notation here chosen (n = 3) for the Rydberg orbitals, in our case these two states are not coupled. Instead, the 1^1E and 2^1E states are coupled, but through the n3s and nσ* configurations (see Table 1); (ii) the nσ* configuration is absent from the results of ref. 11; (iii) the trend obtained for the oscillator strength (*f*) values is significantly different from that here obtained, although in the case of the 2^1E and 1^1A_2 states there is good agreement between our results and that from ref. 11 (see Table 1). In this case the obtained trend for the Rydberg states is $3^1E > 2^1E > 2^1A_1 > 4^1E > 1^1A_2$, while in our case is $2^1E > 4^1E > 3^1E > 2^1A_1 > 1^1A_2$; (iv) the main configuration obtained for the 4^1E state is … $2e^3 5s^1$, while in our case the main configurations are $n3pa_1$ and nσ* (see Table 1). However, Rydberg orbitals with higher *n* values have not been included in our calculations.

As can be seen from Table 1 there is a reasonably good agreement between our *f* values for the nσ* (1^1E) and n3s (2^1E) states and the *f* values obtained experimentally in ref. 45. It is important to mention that an incorrect factor of 1.3 x 10^{-8} was used in this latter reference, instead of 4.39 x 10^{-9}, which should be used for the molar absorption coefficient (ε) in $L.mol^{-1}.cm^{-1}$ [46]. Thus, the experimental *f* values shown in Table 1 have been taken from that of ref. 45 and multiplied by the ratio 4.39 x 10^{-9}/1.3 x 10^{-8}. Although in the case of the $n3pa_1$ state the agreement does

not seem to be good the overlap between the vibrational progression of the previous band (with maximum at 8.89 eV) and the band of the $n3pa_1$ state[9] indicates that the *f* value calculated in ref. 45 is likely to be overestimated. However, the fig.2(b) of ref.9 also indicates that obtaining an accurate *f* value for the $n3pa_1$ band is a very difficult task, due to the overlap between vibrational progressions of adjacent bands. The largest *f* value has been obtained for the 4^1A_1 state, which is compatible with a very broad and intense band, with maximum at 11.64 eV[12]. If one compares the *f* values obtained for the 3^1A_1 and 4^1A_1 states is clear that the very high intensity of the latter band is due to the σσ*configuration (see Table 1).

The additional calculations with the Dunning-Hay DZP + Rydberg" basis set lead to an incorrect description of the 1^1E and 4^1E states at the MR-CISD level, although the results obtained for the other eight states are in reasonable agreement with those shown in Table 1, at this same level. The main configurations obtained for the 1^1E and 4^1E states are $n3pa_1$ and nσ*, respectively, which are not correct. It is important to mention that, although the correct configurations (nσ* and $n3pa_1$, respectively) are not the main configurations, they have non-negligible weights in the wavefunctions obtained for these two states. Further studies are in progress in order to elucidate the reasons for the aforementioned incorrect description.

Table 2 shows the corresponding MCSCF and MR-CISD results (for the singlet states) obtained from the calculations in which only seven states are considered in the state-averaging procedure at the MCSCF level. As can be seen from this table the excitation energies change by at most 0.15, 0.04 and 0.01eV at the MCSCF, MR-CISD and MR-CISD+Q levels, respectively, as compared to the corresponding values of Table 1. The changes in the $\langle r^2 \rangle$ values are practically negligible (compare Tables 1 and 2). Although the *f* values of the two weakest allowed transitions (that is, gs $\rightarrow$ 1^1E and gs $\rightarrow$ 2^1A_1) change significantly the general trend is maintained (compare Tables 1 and 2). The main difference between the results of the two tables is the absence of the $n3pa_1$ configuration in the 1^1E (nσ*) state at the MR-CISD level, although in Table 1 its weight is only 0.17. When a smaller number of states is averaged at the MCSCF level this configuration switches to the 2^1E (n3s) state (see Table 2), at the MR-CISD level. As a consequence the weight of the n3s configuration increases in the 1^1E state and decreases in the 2^1E state (compare Tables 1 and 2). In summary, the highest energy states have a small effect on the properties of the first seven singlet states, at the MR-CISD and MR-CISD+Q levels.

Table 2. MCSCF, MR-CISD, and MR-CISD+Q results for the singlet states of the CH_3Cl molecule, calculated with the mixed aug-cc-pVTZ(H,Cl)/d-aug-cc-pVTZ(C) basis set. Only seven singlet states have been computed.

State						vertical excitation energies[a]		
						MCSCF	MR-CISD	MR-CISD+Q
	weigths (MCSCF)[b]	$\langle r^2 \rangle$[c]	weigths (MR-CISD)[b]	$\langle r^2 \rangle$[c]	E_{tot}[d]	-499.1352011	-499.5199922	-499.565633
1^1A_1	0.96gs	39.86	0.86gs	42.21	*f* (x10^3)[e]	0.00	0.00	0.00
1^1E	0.95(n3s)	84.04	0.58(nσ*)+ 0.23(n3s)	65.74	2.43	6.85	7.52	7.52
2^1E	0.58($n3pa_1$)+0.41(nσ*)	96.33	0.60(n3s)+ 0.14($n3pa_1$)+0.14(nσ*)	76.16	63.79	7.28	7.76	7.88
2^1A_1	0.98(n3pe)	116.07	0.88(n3pe)	113.26	2.78	7.71	8.70	8.88
3^1E	0.98(n3pe)	115.68	0.88(n3pe)	113.32	24.16	7.74	8.71	8.90
1^1A_2	0.98(n3pe)	116.08	0.89(n3pe)	113.69	0.00	7.77	8.75	8.95
4^1E	0.56(nσ*)+0.39($n3pa_1$)	82.90	0.68($n3pa_1$)+0.15(nσ*)	119.75	35.66	8.87	9.21	9.31

[a]in eV; [b]Configurations whose weights are lower than 0.1 were not included; [c]$\langle r^2 \rangle$ expectation values in au; [d]Ground-state energy in hartrees; [e]Oscillator strengths (*f*) calculated at MR-CISD level;

Table 3 shows the results for the nine triplet states studied in the present manuscript. In this case the nature of only two states (1^3E and 2^3E) change as dynamic electron correlation is included, while in the case of the singlet states the nature of 4^1E also changes (see Table 1). Another important difference between the results for triplet and singlet states is the reduced multiconfigurational character for the states of the former multiplicity at the MR-CISD level, a behavior also obtained for some states of the CF_3Cl molecule[5]. For instance, while the weights of the $n3pa_1$ and n3s configurations are negligible in the wavefunction of the 1^3E state they cannot be disregarded in the wavefunction of the 1^1E state (compare Tables 1 and 3). Besides, the Rydberg-valence mixing is greatly reduced in the 1^3E, 2^3E, 4^3E and 3^3A_1 states, which correspond to triplet states whose singlet counterparts have significant multiconfigurational character (compare Tables 1 and 3). Consequently, there is a clear distinction between the average $\langle r^2 \rangle$ values for the valence (~50au), Rydberg 3s (~78au) and Rydberg 3p (~112au) states. For most of the states the effect of dynamic electron correlation in the excitation energies is large, as in the case of the singlet states, except for the 2^3A_1 (σσ*) state (see Table 3). The effect of extensivity correction at MR-CISD+Q level is similar to that obtained for the singlet states, with a maximum increase of 0.24 eV (see Table 3). Through comparison between the excitation energies of the singlet and triplet states is clear that the largest differences have been obtained for the pair of states whose

wavefunctions differ most, that is, for the $5^3E/5^1E$ and $2^3E/2^1E$ pairs at the MCSCF level and for the $5^3E/5^1E$ and $1^3E/1^1E$ pairs at the MR-CISD level (compare Tables 1 and 3). It is important to mention that the 2^3A_1 ($\sigma\sigma^*$) state does not have its singlet counterpart, as for this latter multiplicity the $\sigma\sigma^*$ configuration is of secondary importance in the 4^1A_1 state (see Table 1). Similarly to what has been obtained for the singlet states our MR-CISD+Q values are in good agreement with the corresponding CASPT2 results, although in this case the maximum difference is slightly larger, ~ 0.33 eV, obtained for the 4^3E state. One important difference between our results and the CASPT2 results refers to the energy ordering for the 1^3A_2 and 4^3E states. According to our results at the MR-CISD+Q (and MR-CISD) level $1^3A_2 < 4^3E$, with an energy difference of 0.33 eV, while at the CASPT2 level $4^3E < 1^3A_2$, with an energy difference of only 0.05 eV. As in ref. 10 this ordering does not change as dynamic electron correlation is included (see Table 3).

Table 3. MCSCF, MR-CISD and MR-CISD+Q results for the triplet states of the CH_3Cl molecule, calculated with the mixed aug-cc-pVTZ(H,Cl)/d-aug-cc-pVTZ(C) basis set.

					vertical excitation energies[a]			
state	weigths (MCSCF)[b]	$<r^2>$[c]	weigths (MR-CISD)[b]	$<r^2>$[c]	MCSCF	MR-CISD	MR-CISD+Q	CASPT2[d]
1^3E	0.70(n3s)+0.25(nσ*)	77.35	0.79(nσ*)	53.68	6.55	6.95	6.97	6.70
2^3E	0.42(nσ*)+0.30(n3pa$_1$)+0.27(n3s)	73.89	0.85(n3s)	77.52	6.75	7.59	7.79	7.68
1^3A_1	0.98(n3pe)	112.96	0.88(n3pe)	110.05	7.45	8.55	8.78	8.70
3^3E	0.98(n3pe)	112.95	0.88(n3pe)	110.82	7.54	8.63	8.87	8.81
1^3A_2	0.98(n3pe)	112.97	0.88(n3pe)	111.51	7.62	8.71	8.95	8.90
4^3E	0.64(n3pa$_1$)+0.33(nσ*)	100.02	0.79(n3pa$_1$)	119.62	8.26	8.99	9.18	8.85
2^3A_1	0.90(σσ*)	50.67	0.84(σσ*)	48.13	9.06	9.33	9.37	9.15
3^3A_1	0.96(σ3s)	79.94	0.87(σ3s)	78.58	10.10	10.78	10.87	---
5^3E	0.99(σ3pe)	112.59	0.88(σ3pe)	110.20	10.97	11.81	11.95	---

[a]in eV; [b]Configurations whose weights are lower than 0.1 were not included; [c]$<r^2>$ expectation values in au; [d]ref.[10].

As aforementioned a smaller number (seven) of triplet states have been calculated as well, in order to check how the inclusion of additional states at the MCSCF level affect the MR-CISD and MR-CISD+Q results of these seven states. However, is also important to point out some non-negligible (though small) differences between the results shown in Table 4 and the corresponding results in Table 3 at the MCSCF level. For the sake of consistency the excitation energies in Table 4 are calculated using the ground state singlet energies from Table 2. As can be seen from these tables the valence character of state 1^3E slightly increases while the Rydberg character of the same state slightly decreases (at the MCSCF level), and such changes are accompanied by an increase of the multiconfigurational character of the MCSCF wavefunction (compare Tables 3 and 4). On the other hand, the weight of the nσ* configuration in the 2^3E state slightly decreases, while the weight of the n3s configuration increases substantially, such that this state can be clearly classified as a n3s Rydberg state already at the MCSCF level (compare Tables 3 and 4). At the MR-CISD level only the 2^3E and 4^3E states present non-negligible (though again small) changes in the weights of their configurations, such that these states are now slightly mixed (compare Tables 3 and 4). Small changes have been obtained for the $\langle r^2 \rangle$ values of the seven triplet states. The excitation energies change by at most 0.16, 0.05 and 0.01 eV at the MCSCF, MR-CISD and MR-CISD+Q levels, respectively. Therefore, one can conclude that the inclusion of additional states at the MCSCF level does not alter significantly the main characteristics of the first seven triplet states at the MR-CISD and MR-CISD+Q levels.

Figure 1 below summarizes the best results obtained for the energies of the singlet and triplet states studied for the CH_3Cl molecule.

INSERT FIGURE 1 HERE

Figure 1. Energies (in eV) of the excited singlet and triplet states of the CH_3Cl molecule studied in this manuscript. Only the highest level (MR-CISD+Q) results are shown. Please refer to Tables 1 and 3 for the nature of the excited states.

It is important to mention that the vertical excitation here discussed is, in the Franck-Condon approximation, only the first step in the description of the photodissociation dynamics. Just after the vertical excitation the wavepacket will evolve on the potential energy surface (PES) according to its topography, which controls the photodissociation dynamics. The PES shape is a very important feature to be considered if one wants to understand the type of geometry relaxation adopted by the system during the photodissociation. For instance, after excitation to E states the system (initially in a C_{3v} geometry) has its geometry distorted to Cs or C_1 symmetry (depending on the magnitude of the Jahn-Teller effect), as the C_{3v} ground state geometry belongs to a conical intersection seam. Rydberg states usually relax to equilibrium geometries which are close to the geometry of their ionic core, having a Cs distorted geometry. Other types of geometry relaxations, dictated by the orbitals involved in the electronic excitations, should also be taken into account. For instance, the 1^1E (nσ*) state is also subjected to a breakage of the C-Cl bond. Apart from the geometry relaxations the crossings between electronic states of different nature also govern the photodissociation.

Table 4: MCSCF, MR-CISD, and MR-CISD+Q results for the triplet states of the CH_3Cl molecule, calculated with the mixed aug-cc-pVTZ(H,Cl)/d-aug-cc-pVTZ(C) basis set. Only seven triplet states have been computed.

state					vertical excitation energies[a]		
	weights(MCSCF)[b]	$\langle r^2 \rangle$[c]	weights(MR-CISD)[b]	$\langle r^2 \rangle$[c]	MCSCF	MR-CISD	MR-CISD+Q
1^3E	0.36(nσ*)+0.36(n3pa$_1$)+0.27(n3s)	75.06	0.78(nσ*)	53.31	6.68	6.95	6.96
2^3E	0.64(n3s)+0.33(nσ*)	73.01	0.77(n3s)+0.10(n3pa$_1$)	77.44	6.84	7.62	7.78
1^3A_1	0.98(n3pe)	111.96	0.88(n3pe)	108.96	7.59	8.58	8.78
3^3E	0.98(n3pe)	111.95	0.88(n3pe)	109.76	7.69	8.67	8.87
1^3A_2	0.98(n3pe)	111.96	0.88(n3pe)	110.48	7.78	8.76	8.95
4^3E	0.62(n3pa$_1$)+0.30(nσ*)	104.93	0.69(n3pa$_1$)+0.11(n3s)	120.88	8.34	9.02	9.18
2^3A_1	0.92(σσ*)	48.90	0.84(σσ*)	47.87	9.19	9.36	9.35

[a]in eV; [b]Configurations whose weights are lower than 0.1 were not included; [c]$\langle r^2 \rangle$ expectation values in au.

Conclusions

In this work ten singlet and nine triplet states of the CH_3Cl molecule are studied through multi-reference configuration interaction with singles and doubles (MR-CISD), including Davidson extensivity correction (MR-CISD+Q). The vertical excitation energies, spatial extent ($\langle r^2 \rangle$), configurations weights and oscillator strengths (*f*) have been computed. For the first time the excited states whose energies are larger than ~ 9.5 eV have been calculated using highly correlated methods. At the MR-CISD+Q level the excited states energies vary from ~ 7.51 to

11.98 eV. The lowest (nσ*) excited singlet state is significantly mixed with the $n3p_{a1}$ and n3s Rydberg states, while the next (n3s) has a small admixture with the nσ* state. The next three singlet states obtained result from the $(n_{Cl})^3(3p_e)^1$ configuration and are almost degenerate, with energies of 8.78, 8.87 and 8.90 eV. The next singlet state ($n3p_{a1}$) has a small admixture with the nσ* state, while the last three have $\sigma_{C\text{-}Cl} \rightarrow$ Rydberg (3s or 3p) as the main configurations. According to the *f* values the most intense transition is to the 4^1A_1 state, a $\sigma3p_{a1}$ Rydberg state significantly mixed with the σσ* and σ3s configurations. Our results indicate that the σσ* configuration is responsible for the high *f* value of the gs $\rightarrow 4^1A_1$ transition. The Rydberg-valence mixing is greatly reduced in the triplet states whose singlet counterparts have significant multiconfigurational character. The 2^3A_1 state (σσ*) does not have its singlet counterpart, while the 4^1A_1 state ($\sigma3p_{a1}$ + σσ* + σ3s) does not have its triplet counterpart. The results obtained for the six and seven first singlet and triplet excited states, respectively, are in good agreement with previous CASPT2 results, while in the case of the singlet states some discrepancies with previous MCCEPA results from ref. 11 have been found. Our results are also in good agreement with experimental results from refs. 9 and 12.

Acknowledgments

The authors are thankful to CNPq and CAPES for financial support. They also thank the reviewers for the very valuable suggestions.

Notes and references

[a] *Departamento de Química, CCEN, Universidade Federal da Paraíba, João Pessoa/PB 58059-900 Brazil. Fax: +55 83 3216 7437; Tel: +55 83 3216 7433; E-mail: *elizete@quimica.ufpb.br*

1 M. A. K. Khalil, in: P. Febian, O.N. Singh (Eds.), *The handbook of environmental chemistry*, Part 4E, Reactive Halogen Compounds in the Atmosphere, 52, Springer, Berlin, 1999.
2 (a) M. J. Molina and F. S. Rowland, *Nature,* 1974, **249**, 810; (b) F. S. Rowland and M.J. Molina, *Science,* 1975, **190**, 1038.
3 J. T. G. Hamilton, W. C. McRoberts, F. Keppler, R. M. Kalin and D. B. Harper, *Science,* 2003, **301**, 206.
4 J. R. Lucena Jr., E. Ventura, S. A. do Monte, R. C. M. U. Araújo, M. N. Ramos and R. Fausto, *J. Chem. Phys*., 2007, **127**, 164320.
5 V. C. de Medeiros, E. Ventura and S. A. do Monte, *Chem. Phys. Lett*., 2012, **546**, 30.
6 G. Granucci, G. Medders and A. M. Velasco, *Chem. Phys. Lett*., 2010, **500**, 202.
7 Mei-wen Yen, P. M. Johnson and M. G. White, *J. Chem. Phys*., 1993, **99**, 126.
8 E. Mayor, A. M. Velasco and I. Martin, *J. Phys. Chem. A*, 2004, **108**, 5699.
9 S. Eden, P. Limão-Vieira, S.V. Hoffmann and N.J. Mason, *Chem. Phys.*, 2007, **331**, 232.
10 D. Nachtigallova, D. E. Love and K. D. Jordan, *J. Phys. Chem.*, 1996, **100**, 5642.
11 C. Cossart-Magos, M. Jungen and J. Stalder, *J. Chem. Phys*., 2005, **123**, 104302.
12 R. Locht, B. Leyh, A. Hoxha, H. W. Jochim and H. Baumgärtel, *Chemical Physics*, 2001, **272**, 259.
13 R. Locht, B. Leyh, A. Hoxha, H. W. Jochim and H. Baumgärtel, *Chemical Physics*, 2001, **272**, 277.
14 Z. Shao, H. Li, S. Zhang, J. Li, Z. Dai, Y. Mo, Y. J. Bae and Myung Soo Kim, *J. Chem. Phys*., 2012, **136**, 64308.
15 C. Sándorfy, *The role of Rydberg States in Spectroscopy and Photochemistry*, Kluwer, 2002, chapter 1.
16 G. P. Rodrigues, J. R. Lucena Jr., E. Ventura and S. A. do Monte, *J. Mol. Model*., 2014, **20**, 2393.
17 M. A. F. de Souza, E. Ventura, R. C. M. U. Araújo, M. N. Ramos and S. A. do Monte, *J. Comp. Chem*., 2009, **30**, 1073.
18 R. Locht, B. Leyh, A. Hoxha, H. W. Jochim and H. Baumgärtel, *Chemical Physics*, 2001, **272**, 293.
19 A. W. Potts, H. J. Lempka, D. G. Streets and W. C. Price, *Phil. Trans. R. Soc. Lond. A*, 1970, **268**, 59.
20 P. Jensen, S. Brodersen and G. Guelachvili, *J. Mol. Spect*., 1981, **88**, 378.
21 N. J. Rogers, M. J. Simpson, R. P. Tuckett, K. F. Dunn and C. J. Latimer, *Phys. Chem. Chem. Phys*., 2010, **12**, 10971.
22 I. Antol, M. Eckert-Maksić, T. Müller, M. Dallos and H. Lischka, *Chem. Phys. Lett*., 2003, **374**, 587.
23 A. Bunge, *J. Chem. Phys*., 1979, **53**, 20.
24 S. R. Langhoff and E. R. Davidson, *Int. J. Quantum Chem*., 1974, **8**, 61.
25 P. J. Bruna, S. D. Peyerimhoff and R. J. Buenker, *Chem. Phys. Lett.*, 1981, **72**, 278.
26 H. Lischka, R. Shepard, F.B. Brown and I. Shavitt, *Int. J. Quantum Chem. Symp*., 1981, **15**, 91.
27 R. Sheppard et al., *J. Quantum Chem. Quantum Chem. Symp*., 1988, **22**, 149.
28 H. Lischka, R. Sheppard, I. Shavitt et al., COLUMBUS, an ab initio electronic structure program, Release 7.0, 2012, Institute for Theoretical Chemistry, University of Vienna, Währingerstrasse 17, A-1090, Vienna, Austria.
29 H. Lischka, R. Sheppard, I. Shavitt, R. M. Pitzer, M. Dallos, Th. Müller, P.G. Szalay, M. Seth, G.S. Kedziora, S. Yabushita and Z. Zhang, *Phys. Chem. Chem. Phys*., 2001, **3**, 664.
30 T. Helgaker, H. J. Aa Jensen, P. Jørgensen, J. Olsen, K. Ruud, H. Agren, T. Andersen, K.L. Bak, V. Bakken, O. Christiansen, P. Dahle, E.K. Dalskov, T. Enevoldsen, B. Fernandez, H. Heiberg, H. Hettema, D. Jonsson, S. Kirpekar, R. Kobayashi, H. Koch, K.V. Mikkelsen, P. Norman, M.J. Packer, T. Saue, P.R. Taylor and O. Vahtras, DALTON, an ab initio electronic structure program, Release 1.0, 1997.
31 T.H. Dunning Jr., *J. Chem. Phys*., 1989, **90**, 1007.
32 D. E. Woon and T. H. Dunning Jr., *J. Chem. Phys.*, 1993, **98**, 1358.
33 R. A. Kendall, T. H. Dunning Jr. and R. J. Harrison, *J. Chem. Phys*., 1992, **96**, 6796.
34 T.H. Dunning Jr., D. E. Woon, *J. Chem. Phys*., 1994, **100**, 2975.
35 J.W. Hudgens, T. G. DiGiuseppe and M. C. Lin, *J. Chem. Phys*., 1983, **79**, 571.
36 S. G. Westre, P. B. Kelly, Y. P. Zhang and L. D. Ziegler, *J. Chem. Phys*., 1991, **94**, 270.
37 P. Botschwina, E. Schick and M. Horn, *J. Chem. Phys*., 1970, **53**, 2823.
38 A. M. Mebel and Sheng-Hsien Lin, *Chem. Phys.*, 1997, **215**, 329.
39 T.H. Dunning Jr., *J. Chem. Phys*., 1993, **98**, 9215.

40 T.H. Dunning Jr. and P. J. Hay, in: H. F. Schaefer III (Ed.), *Methods of Electronic Structure Theory*, vol. 2, Plenum Press, New York, 1977.

41 H.-J. Werner, P.J. Knowles, G. Knizia, F.R. Manby, M. Schütz et al., MOLPRO,version 2010.1, a package of ab initio programs.

42 G. P. Rodrigues, J. R. Lucena Jr., E Ventura, S. A. do Monte, I. Reva, and R. Fausto, *J. Chem. Phys*., 2013, **139**, 10.

43 C. A. Theodosiou, M. Inokuti and S. T. Manson, *At. Data Nucl. Data Tables*, 1986, **35**, 473.

44 E. Mayor, A. M. Velasco and I. Martín, *Chem. Phys. Lett.*, 2005, **404**, 35.

45 J. W. Raymonda, L. O. Edwards and B. R. Russell, *J. Am. Chem. Soc*., 1974, **96**, 1708.

46 J. W. Verhoeven, *Pure & Appl. Chem.*, 1996, **68**, 2223.

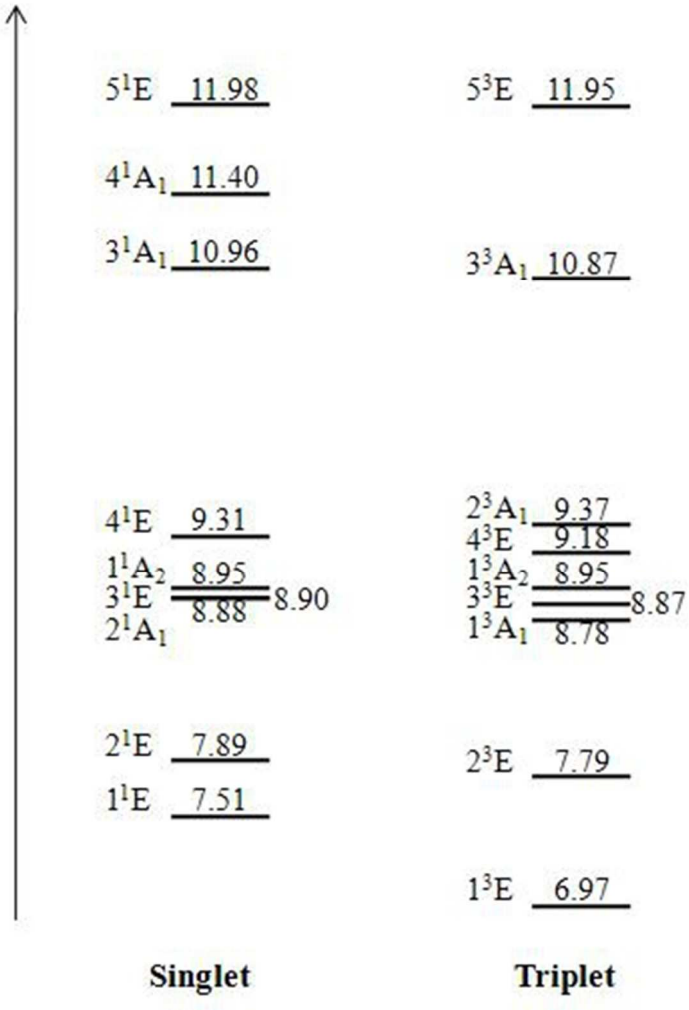

94x134mm (96 x 96 DPI)